Check for updates

# Research on distribution−microgrid-coupled network demand response based on a multi-time scale

Xianglong Zhang[1], Chuang Zhou[2], Yibo Hua[2] and Shufeng Dong[2]*

[1]State Grid Economic and Technological Research Institute Co., Ltd., Beijing, China, [2]College of Electrical Engineering, Zhejiang University, Hangzhou, Zhejiang, China

Under the background of "dual carbon" strategy, the integration of renewable energy adds volatility to the grid. Relying solely on generation-side resources for regulation is inadequate, necessitating a flexible demand response from diverse demandside resources. This paper employs a physical connection and information exchange between the distribution network and microgrids to leverage the advantages of centralized-distributed optimization. This establishes a coordinated demand response model between the distribution network and microgrids, gradually establishing a new type of distribution network that integrates interconnected grids and microgrids. This also necessitates the analysis of the response characteristics of various load resources within microgrids and the categorization and modeling of loads based on their response speeds. Additionally, a method for evaluating the multi-time scale schedulable capacity of microgrids is proposed. Finally, a coordinated demand response model between the distribution network and microgrids based on the schedulable capacity assessment is established. This model is validated through case studies, demonstrating its effectiveness. The coordinated demand response between distribution networks and microgrids enables them to operate in a collaborative and economically safe manner.

## 1 Introduction

The global market is becoming more interconnected due to societal demand and the shift in global industrial development. As a result, climate change and environmental pollution have become increasingly severe issues. The consumption of non-renewable resources in an outdated pattern leads to excessive depletion of finite resources and serious environmental pollution, which constitutes an unsustainable development model. Therefore, the energy transition is currently undergoing continuous experimentation as a strategic approach capable of achieving both improved environmental conditions and resource sustainability (Gielen et al., 2019; Hillerbrand et al., 2019; Li and Kong, 2019).

In China, the power industry accounts for about 40% of the country's carbon emissions (Kang et al., 2022). Under the background of "double carbon," carbon reduction in the power industry has become a key task (Li Y. W. et al., 2022; Zhang and Kang, 2022; Huang

et al., 2023). Opening up new energy and low-carbon transformation is an inevitable trend in the development of the power system. With the continuous improvement of the whole industrial chain system of new energy in China, the construction cost of new energy development has been declining, the pace of market-oriented development of wind power and photovoltaic generation has been accelerating, and the proportion of new energy has gradually increased. At the same time, the impact of uncertain factors such as climate and seasons on new energy generation has brought many new challenges to the power system (Wei, 2019; Li P. S. et al., 2021; Chen, 2021; Yuan et al., 2022; Zhou et al., 2023). It is necessary to fully tap into the diverse resources on the demand side and form a more flexible, convenient, and rapid demand response to improve the regulating capacity of the power system (Jiang, 2018; Gan, 2022).

Microgrids can provide an effective solution to the problems of difficult distributed resource management and insufficient power grid regulation capacity caused by new energy access (Ju and Chen, 2023; Belkhier and Oubelaid, 2024). At the same time, demand response guides users to actively shift and avoid peak loads through market-oriented means (Xu et al., 2018; Wang et al., 2020), which effectively reduce peak loads while also obtaining certain economic benefits for users. It is a win–win approach for the power grid and users.

Demand response is mainly classified into two types: price-based and incentive-based. At present, in the practical application of demand response, users spontaneously adjust their electricity consumption behavior based on the electricity price to obtain benefits from the peak valley dispersion. Large-scale users can obtain corresponding incentives by signing contracts with the power grid to complete the agreed peak load shifting response within the agreed time period. Cui et al. (2021) built the demand response model and guided load adjustments using a price elasticity matrix to alleviate peak system pressures. Li W. et al. (2021) proposed an incentive mechanism for load aggregation merchants targeting shiftable load resources from the perspective of user electricity preferences, thus obtaining optimal incentive contracts for users and optimal scheduling strategies for load aggregation merchants. Both of the above methods fail to closely integrate users' response with grid-side regulation needs, so the response effect often fails to meet expectations. Peak-valley prices are difficult to accurately and dynamically reflect regulation needs, and the scale and frequency of the latter are relatively limited (Fan et al., 2022). For users, the response cost is high and it is difficult to form scale benefits.

Assessing demand response potential is an important aspect of demand response research, also known as the schedulable capacity or controllable capacity. Currently, research on the demand response potential assessment has made some progress (Li et al., 2017; Xu et al., 2017; Zhang et al., 2018), with three typical assessment methods: electricity consumption analysis, elasticity coefficient method, and regression analysis method. Alvarez et al. (2004) quantified the quality and characteristics of its demand response resources through electricity consumption analysis at higher education institutions, achieving a demand response potential assessment at both intraday and intraday time scales. Li et al. (2017) analyzed

the range of load response for industrial, commercial, and residential users based on the electricity demand-price elasticity coefficient, combined with industry load characteristics statistical models, forming a demand response potential envelope. Kong et al. (2022) established a secondary regression parameter database for typical electricity consumption patterns by analyzing key factors influencing power users' participation in demand response, proposing a depth-subdomain adaptive demand response potential assessment method based on feature similarity. The elasticity coefficient assessment method primarily targets load group behaviors with a certain magnitude and is not related to the actual specific load response process. The regression analysis method focuses on users with regular electricity consumption patterns, studying the characteristics and patterns of their historical responses to assess their demand response potential. Both of these methods cannot be used to guide users in conducting demand response.

In addition to theoretical research, countries around the world are actively implementing demand response in practice. The United States has established demand response based on electricity markets in various states, with a wide range of demand response types and relatively well-developed policies and regulations, placing it in a leading position globally. The European Union has not yet formed a comprehensive demand response implementation plan. However, European countries have launched distinctive demand response projects tailored to their national conditions. For instance, France has implemented the "Red, White, and Blue Electricity Price" policy to encourage user participation in demand response. In the United Kingdom, market participants primarily include large electricity users and load aggregation merchants, with transactions executed every half hour and participation in the United Kingdom's electricity balancing mechanism (Huang and Zhang, 2020).

Microgrids not only optimize the coordination of local generation, load, and storage resources to enhance regional economic benefits but also participate as controllable units in the optimization and scheduling at the distribution network level. They provide services such as peak shaving, frequency regulation, and demand response, thereby enhancing grid regulation capabilities and further improving the reliability and flexibility of power system operations (Yang et al., 2014; Dashtdar et al., 2022). Currently, the main application scenarios for coordinated distribution–microgrid operations are optimization and scheduling. Osama et al. (2020) divided large distribution networks into multiple virtual microgrids and proposed a microgrid optimization design method that includes distributed generation units, thereby optimizing the operation and control of the distribution network. Zhou and Ai (2020) studied distribution network systems with multiple microgrids, introducing the concept of a virtual coordinator to divide the topology into a "component–subsystem–main system" structure, achieving a joint economic dispatch of the distribution network and multiple microgrids. Yan et al. (2021) proposed a two-pole network constraint equivalent energy interaction method for multiple microgrids, ensuring flexible connectivity and power exchange between microgrids while maintaining the privacy of microgrids and the operational safety of the distribution network.

As an independent demand-side stakeholder, microgrid-related research studies on the demand response characteristics are relatively well-established, with some explorations and innovations in coordinated distribution-microgrid demand response. Li X. et al. (2022) considered various types of microgrid demand response characteristics and proposed a distributed optimization scheduling strategy for urban distribution systems, reducing overall operating costs and improving the economic viability of microgrids and distribution systems. Li Z. K. et al. (2022) introduced a dual-layer scheduling model considering microgrid demand response and power exchange, with the lower layer coordinating the outputs of various microgrids to minimize operating costs, while the upper layer optimizes active and reactive power at the distribution network level. Kahnamouei and Lotfifard (2022) achieved a critical load recovery after extreme events through the coordinated optimization of distributed energy sources, microgrids, and demand response.

However, current research studies have not fully utilized the function of distribution networks as guideline for the demand response of microgrids nor has it distinguished the demand response of microgrids from other stakeholders at the practical application level. If the guidance role of the distribution network on microgrid demand response can be strengthened, forming a dedicated channel for coordinated demand response between distribution and microgrids, where microgrid demand response becomes the execution of "demand response instructions" from the distribution network, it can achieve more targeted and frequent small-scale demand response. Additionally, it would exhibit characteristics of being more stable, accurate, and rapid in response.

Therefore, this paper conducts research on the distribution–microgrid-coordinated demand response based on the multi-time scale schedulability assessment. Conducting specific application scenario research on coordinated distribution–microgrid demand response, this paper aims to enhance the rapid regulation capabilities of distribution networks through scaled and normalized microgrid demand response, thereby forming a hierarchical demand response structure. The contributions of this study are as follows:

(1) Proposed a load grading modeling method based on the response time of loads. By considering the different response characteristics of different loads within the microgrid, especially their response time during demand response, a load grading modeling method was proposed. The grading of loads corresponds to demand response at multiple time scales.

(2) Introduced a multi-time scale dispatching ability assessment method for microgrids. Based on the grading model, demand response was divided into four scales: day-ahead, hourly, minute-level, and second-level. A multi-time scale dispatching ability assessment model for microgrids was established to describe the relationship between schedulable loads and corresponding costs.

(3) Studied distribution–microgrid coordinated demand response based on the multi-time scale schedulable capacity assessment. Leveraging the load grading model and multi-time scale schedulable capacity assessment of

microgrids, a distribution–microgrid coordinated demand response framework was developed. This framework maximizes the advantages of centralized-distributed optimization, allowing rapid instructions from the distribution network to the microgrid for stable and accurate responses. This approach achieves stable and efficient demand response while maximizing economic benefits.

# 2 Load classification and modeling considering response time

First, the response time, sustainability time, response uncertainty, and differential characteristics of demand response of commonly available demand response loads are studied, and the load is divided into seven levels according to response time, as shown in Figure 1. Different levels of load resources can meet the regulatory needs of different scenarios. Below is a load modeling of interruptible loads, energy storage, electric vehicles, and air conditioning that this article focuses on, and a brief explanation of their control methods of how they involve in demand response.

## 2.1 Interruptible loads

Interruptible loads can be controlled through load control devices such as specialized transformer load control terminal or precise load control terminal to achieve shunt tripping function and complete load control. The response time is less than 1 s, and it belongs to the first-level response resources.

$$P_{IL-DR,t} = Z_{IL,t}P_{IL,t}, \tag{1}$$

where $P_{IL,t}$ is the power before interruptible load response; $Z_{IL,t}$ is a binary variable (0 or 1) that enables the interruption of interruptible loads, where 0 indicates the removal of interruptible loads and 1 indicates the normal operation of interruptible loads; and $P_{IL-DR,t}$ is the power of interruptible loads considering demand response.



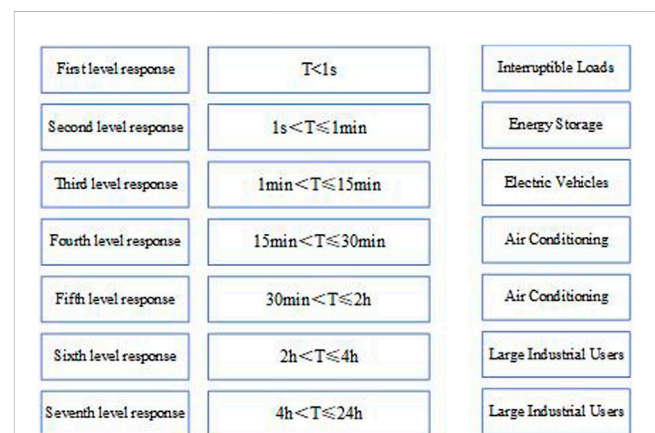| First level response | T<1s | Interruptible Loads |
| Second level response | 1s<T≤1min | Energy Storage |
| Third level response | 1min<T≤15min | Electric Vehicles |
| Fourth level response | 15min<T≤30min | Air Conditioning |
| Fifth level response | 30min<T≤2h | Air Conditioning |
| Sixth level response | 2h<T≤4h | Large Industrial Users |
| Seventh level response | 4h<T≤24h | Large Industrial Users |

FIGURE 1
Load grading by response time.

## 2.2 Energy storage

The energy storage can flexibly adjust the charge–discharge power according to the power command, achieving a bidirectional power flow and fast response. The response time is in the second level, so the energy storage belongs to the second-level response resources. Then, a load model for energy storage is established:

$$P_{BESS,t} = P_{bc,t} - P_{bd,t}, \tag{2}$$

$$SOC_{t+1} = SOC_t + \left( \eta_{bc} P_{bc,t} \Delta t - \frac{P_{bd,t}}{\eta_{bd}} \Delta t \right) \Big/ S_b, \tag{3}$$

$$SOC_{\min} \leq SOC_t \leq SOC_{\max}, \tag{4}$$

$$P_{bc,\min} \leq P_{bc,t} \leq P_{bc,\max}, \tag{5}$$

$$P_{bd,\min} \leq P_{bd,t} \leq P_{bd,\max}, \tag{6}$$

where $P_{BESS,t}$ is the output power of energy storage equipment at time $t$ in microgrids, and a positive value indicates charging, while the negative one indicates discharging. $P_{bc,t}$ and $P_{bd,t}$ are charge power and discharge power of the energy storage at time $t$, respectively; $\eta_{bc}$ and $\eta_{bd}$ are the charge–discharge efficiency of the energy storage, respectively; $\Delta t$ represents the charging and discharging time, and here, it is set to 1; $S_b$ is the capacity of the energy storage; $SOC_t$ is the state of charge (SOC) for energy storage at time $t$; Eqs 4–6 indicate the restrain of SOC and charge–discharge power; $SOC_{\max}$ and $SOC_{\min}$ are the upper and lower limits of SOC, respectively; $P_{bc,\max}$ and $P_{bc,\min}$ are the upper and lower limits of charge power, respectively; and $P_{bd,\max}$ and $P_{bd,\min}$ are the upper and lower limits of discharge power for energy storage, respectively.

## 2.3 Electric vehicles

The electric vehicles can be regarded as the user's private and movable energy storage. To achieve a two-way power flow, special charging station equipment is required and complex practical factors such as ownership, battery loss, financial compensation, and user willingness are considered. More technical and policy supports are needed in the actual application; therefore, this paper only considered the charging properties of electric vehicles which conducted demand response by stopping charging. The response time is approximately 5–15 min, which belongs to the third-level response resources.

User $j$ could choose to accept a set of charging interruption periods, denoted as $T_{st,j} = \{t_1, t_2, \ldots, t_n\}$, as well as the maximum duration of charging interruption, $T_{EV,j}$, to establish a load model for electric vehicles:

$$P_{EV-DR,j,t} = Z_{EV,j,t} P_{EV,j,t}, \tag{7}$$

$$\mathbf{Z_{EV,j}} = \left[ Z_{EV,j,1}, Z_{EV,j,2}, \ldots, Z_{EV,j,T} \right], \tag{8}$$

$$Z_{EV,j,t} = 1, t \notin T_{st,j}, \tag{9}$$

$$\sum_{t=1}^{T} \left( 1 - Z_{EV,j,t} \right) \leq T_{EV,j}, \tag{10}$$

where $P_{EV,j,t}$ represents the power of electric vehicle load $j$ before response; $P_{EV-DR,j,t}$ represents the power of electric vehicle load considering demand response; $Z_{EV,j,t}$ is a binary variable (0 or 1) that controls the start/stop charging of electric vehicle load, where 0 indicates charging interruption and 1 indicates the resumption of normal charging; $\mathbf{Z_{EV,j}}$ is a vector form of the binary variable for $T$ time periods; $T$ represents a demand response cycle; Eq. 9 represents the constraint for periods without participating in demand response; and Eq. 10 represents the constraint for the maximum duration of charging interruption.

## 2.4 Air conditioning

Air conditioning is a typical temperature-controlled load, and its operation characteristics are closely related to the thermal changes in buildings. Buildings have certain thermal storage properties, and human comfort temperature is within a range, which gives air conditioning loads a virtual energy storage property. The temperature adjustment lag makes the response time of air conditioning in the order of hours, making it a fourth- or fifth-level response resource. Then, a load model for air conditioning is established:

$$Q_{AC,t} = \eta_{AC} P_{AC,t}, \tag{11}$$

$$c_a \rho_a V (\theta_{t+1} - \theta_t) = \left( Q_{gain,t} - Q_{AC,t} \right) \Delta t, \tag{12}$$

$$Q_{gain,t} = \alpha_a S_a \left( \theta_{out,t} - \theta_t \right), \tag{13}$$

$$P_{AC,\min} \leq P_{AC,t} \leq P_{AC,\max}, \tag{14}$$

where $P_{AC,t}$ represents the power consumption of the air conditioning system. $\eta_{AC}$ is the energy efficiency ratio (EER) of the air conditioning system. $Q_{AC,t}$ represents the cooling power of the air conditioning system; Eq. 12 represents the heat conduction formula for the buildings, where $c_a$ is the specific heat capacity of air, $\rho_a$ is the density of air, $V$ is the volume of the buildings, $\theta_t$ is the indoor temperature at time t, and $\Delta t$ represents the heat exchange time, and here, it is set to 1. $Q_{gain,t}$ represents the heat gained by the buildings due to the temperature difference, where $\alpha_a$ is the heat transfer coefficient, $S_a$ is the surface area of the buildings, and $\theta_{out,t}$ is the outdoor temperature. $P_{AC,\max}$ and $P_{AC,\min}$ represent the upper and lower limits of the power consumption of the air conditioning system, respectively. These limits can be set based on the capacity and operational constraints of the air conditioning system.

## 3 Evaluation of microgrid's multi-time scale dispatching ability

The dispatching ability of a microgrid refers to the relationship between the reduction amount and corresponding cost in a specific future time period based on the planned/current operating state of the microgrid (Wang, 2020; Xu, 2021). Depending on the time scale, it can be categorized into day-ahead, hourly, minute, and second dispatching abilities.

The evaluation process of the multi-time scale dispatching ability of a microgrid and its specific application scenarios are illustrated in Figure 2.

At the day-ahead time scale, the microgrid conducts economic optimization based on time-of-use electricity prices to meet the energy

demand of users to the greatest extent. Only the generation units and energy storage output are optimized, and the planned electricity consumption curve is reported to the distribution network. The distribution network then issues day-ahead demand response periods based on the overall situation. The microgrid evaluates its day-ahead dispatching ability for demand response periods and reports it to the distribution network. Day-ahead demand response ensures the energy demand of users and is achieved solely through generation units and energy storage resources. The distribution network performs coordinated optimization based on the dispatching ability of each microgrid and issues demand response instructions to each microgrid. The microgrid then conducts day-ahead optimization, considering the demand response based on the instructions.

At the intraday time scale, the microgrid operates normally based on the day-ahead optimization results while conducting minute and second dispatching ability evaluations, which are updated every 15 min. When the distribution network issues hourly demand response periods, the microgrid evaluates its hourly dispatching ability for the specific period and reports it to the distribution network. Hourly demand response sacrifices a portion of user satisfaction with energy consumption and involves not only generation units and energy storage resources but also air conditioning and electric vehicles. After coordinated optimization by the distribution network, demand response instructions are issued to the

microgrid, and the microgrid performs hourly demand response accordingly. When the distribution network issues minute-level demand response instructions, the microgrid executes pre-set minute-level demand response coordination strategies, which are achieved through electric vehicles and energy storage with minute-level response speeds. When the distribution network issues second-level demand response instructions, the microgrid's load controller automatically executes the corresponding instructions, involving interruptible loads and energy storage with second-level response speeds.

In summary, different time scales of demand response involve different resources. The day-ahead grid side has more diverse regulation measures, so the microgrid side participates in day-ahead demand response while meeting the energy needs of users, utilizing generation units and energy storage as response resources. For the overall grid, the dispatchable day-ahead resources are relatively limited. Therefore, the microgrid sacrifices a portion of users' satisfaction to increase the response quantity, mobilizing all resources that can meet the response speed for intraday demand response. Hourly demand response involves generation units, air conditioning, electric vehicles, and energy storage. A minute-level demand response involves electric vehicles and energy storage. The second-level demand response only considers energy storage and interruptible loads.
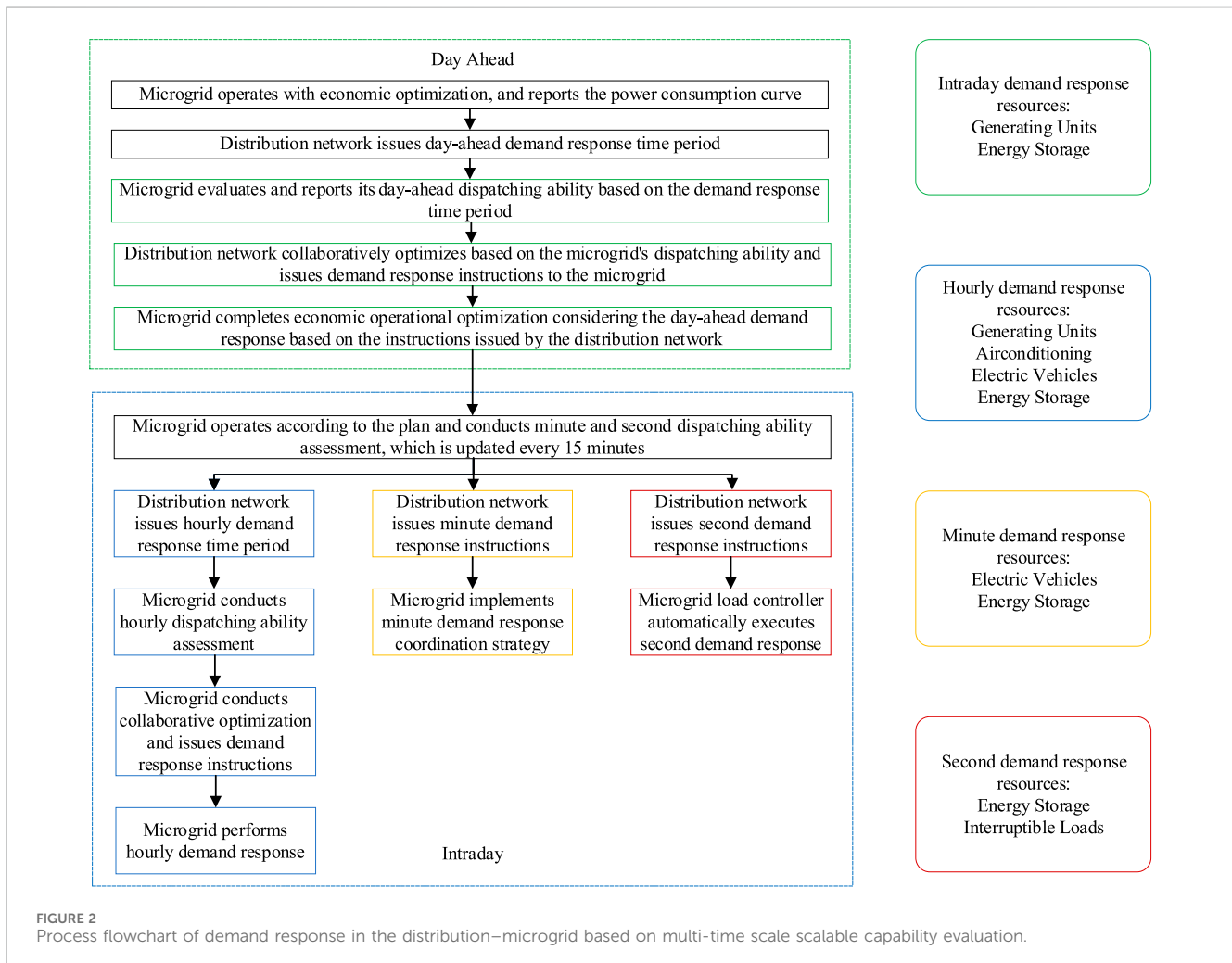


FIGURE 2
Process flowchart of demand response in the distribution−microgrid based on multi-time scale scalable capability evaluation.

## 3.1 Economic operation of microgrids

The economic optimization results of microgrid operation in the day-ahead grid size are used as the basis for dispatching ability evaluation. Every day is divided into $T = 96$ time intervals, with each interval being $\Delta t = 15$ min. The microgrid optimizes energy consumption based solely on time-of-use electricity prices, with the objective of minimizing internal daily operating costs. The decision variables include microgrid purchasing power, generation unit output, and energy storage output shown in Eq. 15 to Eq. 18. The objective function is defined as follows:

$$\min C_{MG} = C_e + C_G + C_{om}, \tag{15}$$

where $C_{MG}$ represents the daily operating cost of the microgrid, $C_e$ represents the purchasing cost of electricity for the microgrid, $C_G$ represents the generation cost of the internal generation units in the microgrid, and $C_{om}$ represents the cost of equipment operation and maintenance.

$$C_e = \sum_{t=1}^{T} (c_{e,t} P_{M-D,t}) \Delta t, \tag{16}$$

where $c_{e,t}$ represents the time-of-use electricity price and $P_{M-D,t}$ represents the power exchanged between the microgrid and the distribution network at time $t$, which is the power purchased by the microgrid from the distribution network.

$$C_G = \sum_{t=1}^{T} \sum_{j=1}^{N_G} (a_{G,j} P_{G,j,t}^2 + b_{G,j} P_{G,j,t} + c_{G,j}) \Delta t, \tag{17}$$

where $P_{G,j,t}$ represents the output of generation unit $j$ in the microgrid at time $t$. $a_{G,j}$, $b_{G,j}$, and $c_{G,j}$ are the corresponding cost coefficients for the generation unit. $N_G$ represents the number of generation units in the microgrid.

$$C_{om} = \sum_{t=1}^{T} (c_{om,AC} P_{AC,t} + c_{om,BESS} |P_{BESS,t}|) \cdot \Delta t, \tag{18}$$

where $c_{om,AC}$ represents the unit power operation and maintenance cost for air conditioning and $c_{om,BESS}$ represents the unit power operation and maintenance cost for energy storage.

The power balance constraint, generation unit output and ramping constraints, equipment constraints, and environmental temperature constraints in the microgrid are expressed as follows from Eq. 19 to Eq. 22:

(1) Power balance constraint:

$$P_{M-D,t} = P_{IL,t} + P_{BESS,t} + \sum_{j=1}^{N_{EV}} P_{EV,j,t} + P_{AC,t} + P_{L,t} - P_{PV,t} - \sum_{j=1}^{N_G} P_{G,j,t}, \tag{19}$$

where $P_{L,t}$ represents the power of other non-dispatchable loads in the microgrid and $P_{PV,t}$ represents the output power of the photovoltaic system.

(2) Generation unit output and ramping constraints:

$$P_{G,j,\min} \leq P_{G,j,t} \leq P_{G,j,\max}, \tag{20}$$

$$|P_{Gj,t} - P_{Gj,t-1}| \leq r_{Gj,\max} \Delta t, \tag{21}$$

where $P_{G,j,\max}$ and $P_{G,j,\min}$ represent the upper and lower limits of the generation unit $j$'s output, respectively. $r_{Gj,\max}$ represents the maximum ramping rate of the generation unit.

(3) Equipment constraints:>Eqs 1–14
(4) Environmental temperature constraints:

$$\theta_{set,\min} \leq \theta_t \leq \theta_{set,\max}, \tag{22}$$

where $\theta_{set,\max}$ and $\theta_{set,\min}$ represent the upper and lower limits of the indoor environmental temperature, which are typically set to default values $\theta_{\max}$ and $\theta_{\min}$, respectively. However, during hourly demand response, they can be adjusted. When the environmental temperature exceeds the range of human comfort, an environmental temperature penalty is applied to compensate for the decrease in user satisfaction due to reduced comfort.

## 3.2 Day-ahead dispatching ability evaluation

Day-ahead dispatching ability (DADA) refers to the relationship between the achievable reduction amount and the corresponding cost in the known day-ahead demand response time period $T_{DR-D} = \{t_1, t_2, \ldots, t_n\}$ for a microgrid. The expression for DADA is given by Eq. 23:

$$C_{DR-D} = f_{DR-D} (n \cdot \Delta P_{DR-D}), \tag{23}$$

where $f_{DR-D}$ represents the function that describes the relationship between the reduction amount and the corresponding cost in the day-ahead demand response. $\Delta P_{DR-D}$ represents the unit reduction amount in the day-ahead demand response. $n$ is a positive integer used to represent the increasing steps of the reduction amount. $C_{DR-D}$ represents the cost increase associated with the corresponding reduction amount. The relationship equation is obtained through the following steps:

Step 1: Perform day-ahead economic optimization to obtain the microgrid's daily operating cost without considering the demand response, denoted as $C_{MG,DR-D,0} = C_{MG}$. Given the day-ahead demand response time period $T_{DR-D} = \{t_1, t_2, \ldots, t_{n_{DR-D}}\}$, set the unit reduction amount as $\Delta P_{DR-D}$ and set an initial value for $n = 1$.

Step 2: Add the reduction amount constraint to the microgrid's economic operation optimization problem in Section 2.1, as shown in the following Eq. 24:

$$P_{M-D,t}^{DR-D} \leq P_{M-D,t} - n \cdot \Delta P_{DR-D}, t \in T_{DR-D}, \tag{24}$$

where $P_{M-D,t}^{DR-D} \leq P_{M-D,t} - n \cdot \Delta P_{DR-D}, t \in T_{DR-D}$ represents the planned purchasing power from the microgrid to the distribution network after day-ahead demand response and $P_{M-D,t}^{DR-D} \leq P_{M-D,t} - n \cdot \Delta P_{DR-D}, t \in T_{DR-D}$ represents the planned purchasing power obtained from day-ahead economic optimization.

Step 3: The decision variables are the microgrid's purchasing power and the output of generation units and energy storage. Solve the optimization problem.

Step 4: If the optimization problem has a solution, obtain the microgrid's daily operating cost $C_{MG,DR-D,n}$ corresponding to the reduction amount $\cdot \Delta P_{DR-D}$. Calculate the cost increase of demand response $C_{DR-D,n}$ using Eq. 25, and set $n = n + 1$. Repeat steps 2 and 3. If

there is no solution, obtain the maximum achievable reduction amount in day-ahead demand response $(n-1) \cdot \Delta P_{DR-D}$ and proceed to step 5.

$$C_{DR-D,n} = C_{MG,DR-D,n} - C_{MG,DR-D,0}. \tag{25}$$

Step 5: Based on the obtained $n$ sets of data: $\{(n \cdot \Delta P_{DR-D}, C_{DR-D,n})|n \in N_D\}$, where $N_D$ is the set of values for which the optimization problem has a solution, approximate the relationship between the reduction amount and the corresponding cost as linear between adjacent sets of data. This allows for the solution of the relationship equation $C_{DR-D} = f_{DR-D}(n \cdot \Delta P_{DR-D})$.

## 3.3 Hourly dispatching ability evaluation

Hourly dispatching ability (HDA) refers to the relationship between the achievable reduction amount and the corresponding cost in the hourly demand response time period $T_{DR-H} = \{t_1, t_2, ..., t_{n_{DR-H}}\}$ for a microgrid. The expression for HDA is given by Eq. 26:

$$C_{DR-H} = f_{DR-H}(n \cdot \Delta P_{DR-H}). \tag{26}$$

The parameters in the equation have the same meanings as in the day-ahead dispatching ability, and the solution steps are also the same as in the day-ahead evaluation method, so it will not be repeated. The final result is a set of data denoted as $\{(n \cdot \Delta P_{DR-H}, C_{DR-H,n})|n \in N_H\}$. The difference lies in the decision variables, which include not only the microgrid's purchasing power and the output of generation units and energy storage but also the output of air conditioning and the binary variable $\mathbf{Z_{EVj}}$ for electric vehicles. To increase the hourly dispatching ability of the microgrid, the upper and lower limits of the environmental temperature, $\theta_{max}$ and $\theta_{min}$, can be set to fully utilize the hourly response speed of the air conditioning load. The participation of air conditioning and electric vehicles in demand response will decrease user satisfaction, so compensation terms need to be added to the original objective function, shown in Eq. 27 to Eq. 29:

$$\min C_{MG} = C_e + C_G + C_{om} + C_\theta + C_{EV}, \tag{27}$$

where $C_\theta$ represents the compensation for environmental temperature and $C_{EV}$ represents the compensation for the participation of electric vehicles in demand response.

(1) Environmental temperature cost:

$$C_\theta = \sum_{t=1}^{T} c_\theta \left[ Z_{\theta up}(\theta_t - \theta_{max}) + Z_{\theta down}(\theta_{min} - \theta_t) \right] \cdot \Delta t, \tag{28}$$

where $c_\theta$ represents the penalty unit price for temperature, $Z_{\theta up}$ and $Z_{\theta down}$ are binary variables (0 or 1) indicating whether the temperature exceeds the upper or lower limit. A value of 0 indicates that the temperature is within the limit, while a value of 1 indicates that the temperature has exceeded the limit. $\theta_{max}$ and $\theta_{min}$ represent the upper and lower limits of the human comfort temperature, respectively.

(2) Electric vehicle compensation:

$$C_{EV} = \sum_{t=1}^{T} \sum_{j=1}^{N_{EV}} c_{EV-DR,t} \left( P_{EV,j,t} - P_{EV-DR,j,t} \right) \cdot \Delta t, \tag{29}$$

where $N_{EV}$ represents the number of charging stations in the microgrid and $c_{EV-DR,t}$ represents the unit compensation price for electric vehicles to stop charging.

## 3.4 Minute dispatching ability evaluation

Minute dispatching ability (MDA) refers to the relationship between the achievable reduction amount and the corresponding cost in the minute-level demand response for a microgrid. The expression for MDA is given by Eq. 30:

$$\left\{ (n \cdot \Delta P_{DR-M}, C_{DR-M,n})|n \in N_M \right\}. \tag{30}$$

The solution steps and the evaluation methods are consistent with the previous approach and will not be reiterated. The differences are as follows: 1) instead of solving for specific time periods, the solution will be for the 1-h time period 30 min later, with updates every 15 min; 2) the power generation units and air conditioning load will remain in their planned operating state without control adjustments, and the optimization decision variables will be the energy storage output and the binary variable $\mathbf{Z_{EV,j}}$ for electric vehicles; 3) the minute-level dispatchable capacity will no longer be represented by a relationship curve between the reduction amount and corresponding cost but will provide a fixed set of optional reduction amounts; and 4) the optimization results corresponding to each set of reduction amounts will be saved, allowing the microgrid to execute the corresponding minute-level demand response strategy when the distribution network issues minute-level demand response instructions.

## 3.5 Second dispatching ability evaluation

The second dispatching ability refers to the maximum reduction amount that a microgrid can achieve in second-level demand response, without considering costs. The calculation method is as follows in Eqs 31–33:

$$\Delta P_{DR-S} = P_{IL,t} + \Delta P_{BESS,DR-S}, \tag{31}$$

$$\Delta P_{BESS,DR-S} = P_{BESS,t} - P_{bd,DR-S}, \tag{32}$$

$$P_{bd,DR-S} = \min \left\{ P_{bd,max}, \frac{(SOC_t - SOC_{min}) \cdot S_b \cdot \eta_{bd}}{\Delta t} \right\}, \tag{33}$$

where $\Delta P_{DR-S}$ represents the maximum reduction amount in second-level demand response, including the maximum adjustment power of interruptible loads and energy storage. $\Delta P_{BESS,DR-S}$ represents the maximum adjustment power of energy storage, which is obtained by subtracting the maximum discharge power $P_{bd,DR-S}$ after the response from the energy storage output before the response. The maximum discharge power $P_{bd,DR-S}$ should be sustained for at least $\Delta t$.

When the distribution network issues a second-level demand response instruction, the load controller within the microgrid automatically executes the corresponding instruction. It disconnects the interruptible loads and simultaneously initiates the discharge of the energy storage system at the maximum discharge power until it reaches $SOC_{min}$.

# 4 Distribution–microgrid-coupled network demand response

## 4.1 Day-ahead and hourly demand responses

At the day-ahead level, the distribution network receives the power consumption plan curve $P_{D-M,i,t}$ reported by each microgrid $i$, which is the economic operation optimization result of the microgrid, as mentioned in Section 2.1. After assessing the overall energy usage of the system for safety, the distribution network sends a day-ahead demand response invitation to the microgrid, during $T_{DR-D} = \{t_1, t_2, ..., t_{n_{DR-D}}\}$. Microgrid $i$ reports its day-ahead dispatching ability for the corresponding time period to the distribution network. The distribution network performs economic dispatch, considering the dispatching capacity and cost of each microgrid, taking into account the constraints for safe operation of the power lines. It calculates the reduction amount for each microgrid and sends it to the respective microgrid. The microgrid then responds during the specified time period, completing the day-ahead demand response coordinated between the distribution network and microgrid. The formulation of the coordinated demand response model between the distribution network and microgrid is consistent for both the previous day and hourly levels. This section will use the previous day as an example for illustration.

The objective function is to minimize the operating cost of the distribution network and the interaction cost between the distribution network and the microgrid. The decision variables are the power generation output of the units and the demand response quantity of the microgrid. The objective function can be expressed as follows in Eqs 34–37:

$$\min C_{DN} = C_{T-D} + C_{D-G} - C_{D-M}, \quad (34)$$

where $C_{T-D}$ represents the purchasing cost of the distribution network from the transmission network, $C_{D-G}$ represents the generation cost of the distribution network, and $C_{D-M}$ represents the interaction cost between the distribution network and the microgrid.

(1) Distribution network electricity procurement cost:

$$C_{T-D} = \sum_{t=1}^{T_1} c_{Te,t} P_{T-D,t}, \quad (35)$$

where $c_{Te,t}$ represents the electricity price for purchasing by the distribution network, $P_{T-D,t}$ represents the purchasing power of the distribution network from the transmission network at time $t$, and $T_1$ represents the demand response time period.

(2) Distribution network generation cost:

$$C_{D-G} = \sum_{t=1}^{T_1} \sum_{j=1}^{N_{D-G}} \left( a_{D-G,j} P_{D-G,j,t}^2 + b_{D-G,j} P_{D-G,j,t} + c_{D-G,j} \right) \Delta t, \quad (36)$$

where $P_{D-G,j,t}$ represents the output of the power generation unit $j$ in the distribution network at time $t$. $a_{D-G,j}$, $b_{D-G,j}$, and $c_{D-G,j}$ are the corresponding cost coefficients for the power generation unit $j$. $N_{D-G}$ represents the number of power generation units in the distribution network.

(3) Interactions cost between the distribution network and microgrid:

$$C_{D-M} = \sum_{i=1}^{N_{MG}} f_{DR-D,i}\left( P_{DR-D,i}^{cmd} \right), \quad (37)$$

where $P_{DR-D,i}^{cmd}$ represents the demand response peak shaving instruction issued by the distribution network to the microgrid $i$. $f_{DR-D,i}\left( P_{DR-D,i}^{cmd} \right)$ represents the corresponding cost increase for the microgrid $i$ when the reduction amount is $P_{DR-D,i}^{cmd}$.

The power balance constraint of the distribution network, line flow constraints, unit output and ramping constraints, and reduction amount constraints are expressed as follows Eqs 38–43:

(1) Power balance constraints:

$$P_{T-D,t} + \sum_{j=1}^{N_{D-G}} P_{D-G,j,t} = \sum_{i=1}^{N_{MG}} P_{D-M,i,t} + \sum_{n=1}^{N_L} P_{D-L,n,t}, \quad (38)$$

where $P_{D-L,n,t}$ represents the power consumed by the uncontrollable load at the $n$ th location in the distribution network at time $t$.

(2) Line-flow constraints:

$$S_{l,\min} \leq S_{l,t} \leq S_{l,\max}, \quad (39)$$

$$S_{l,t} = \sum_{j=1}^{N_{D-G}} H_{l-j} P_{D-G,j,t} + \sum_{i=1}^{N_{MG}} H_{l-i} P_{D-M,i,t} + \sum_{n=1}^{N_L} H_{l-n} P_{D-L,n,t}, l \in N_L, \quad (40)$$

where $S_{l,t}$ represents the power flow through the transmission line $l$ in the distribution network at time $t$. $S_{l,\max}$ and $S_{l,\min}$ represent the upper and lower limits of the power flow through the line $l$, respectively. $H_{l-j}$, $H_{l-i}$, and $H_{l-n}$ represent the power transmission distribution factors (PTDF) corresponding to the power generation unit $j$, microgrid $i$, and uncontrollable load $n$, respectively. $N_L$ represents the set of transmission lines in the distribution network.

(3) Unit output and ramping constraints:

$$P_{D-G,j,\min} \leq P_{D-G,j,t} \leq P_{D-G,j,\max}, \quad (41)$$

$$\left| P_{D-G,j,t} - P_{D-G,j,t-1} \right| \leq r_{D-G,j,\max} \Delta t, \quad (42)$$

where $P_{D-G,j,\max}$ and $P_{D-G,j,\min}$ represent the upper and lower limits of the power generation output for unit $j$, respectively. $r_{D-G,j,\max}$ represents the maximum ramping rate for unit $j$.

(4) Reduction amount constraints:

$$\sum_{i=1}^{N_{MG}} P_{DR-D,i}^{cmd} \geq P_{DR}, \quad (43)$$

where $P_{DR}$ represents the total reduction amount requirement for the distribution network.

By solving the above optimization problem, we can obtain the reduction amount $\left\{ P_{DR-D,1}^{cmd}, P_{DR-D,2}^{cmd}, ..., P_{DR-D,N_{MG}}^{cmd} \right\}$ for each microgrid.
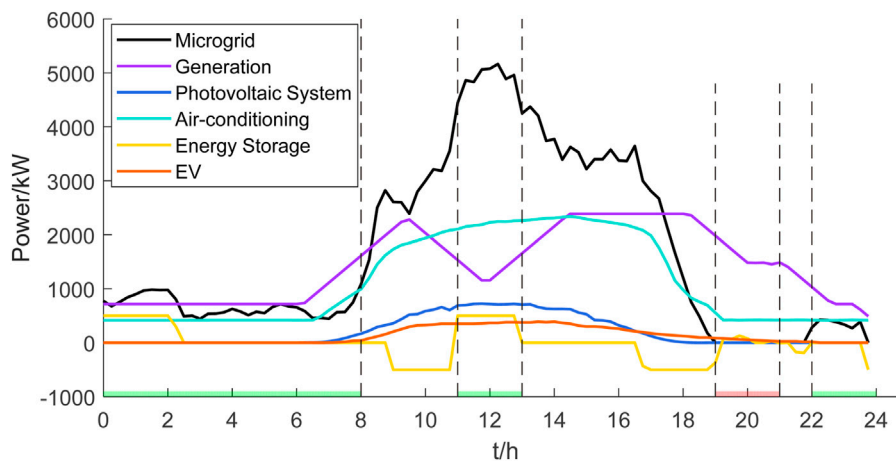
**FIGURE 3**
Day-ahead economic operation curve of Microgrid 1.

## 4.2 Minute and second demand response

During the minute demand response coordinated between the distribution network and microgrid, considering the requirement for response speed, the reported dispatching ability of microgrid $i$ is no longer a relationship curve between the reduction amount and corresponding cost. Instead, it is a fixed set of reduction amounts $\{(n \cdot \Delta P_{DR-M,i}, C_{DR-Mn,i}) | n \in N_{M,i}\}$. The distribution network optimizes its operation to determine the reduction amount for each microgrid $\{n_1 \cdot \Delta P_{DR-M,1}, n_2 \cdot \Delta P_{DR-M,2}, ..., n_{N_{MG}} \cdot \Delta P_{DR-M,N_{MG}} | n_i \in N_{M,i}\}$.

During a second demand response coordinated between the distribution network and microgrid, the reported second dispatching ability by the microgrid is denoted as $\Delta P_{DR-S,i}$. The microgrids are sorted based on the reduction amount in descending order, and the microgrid index is denoted as $\{x_1, x_2, ..., x_{N_{MG}}\}$. Given the requirement to meet the second reduction amount $P_{DR-S}$, the distribution network determines the participating users $\{x_1, x_2, ..., x_{NS}\}$ for second demand response based on the "capacity priority" principle, satisfying the following equation in Eqs 44, 45:

$$\sum_{x=x_1}^{x_{NS}-1} \Delta P_{DR-S,x} \leq P_{DR-S,} \qquad (44)$$

$$\sum_{x=x_1}^{x_{NS}} \Delta P_{DR-S,x} \geq P_{DR-S}. \qquad (45)$$

## 5 Examples

The calculations will be performed on a computer with an Intel Core i7-12700 2.10 GHz processor and 16 GB of memory. The programming language used will be MATLAB R2019a, and the CPLEX 12.10 solver will be invoked for solving the optimization problem.

## 5.1 Analysis of the dispatching ability

The evaluation and analysis of the dispatchable capacity at different time scales were conducted for Microgrid 1 during the time period of 15: 00–17:00. Figure 3 presents the economic operation results of Microgrid 1 in advance. The various regions of time-of-use electricity prices are indicated by dashed lines and colors at the bottom of the x-axis. The green color represents the off-peak electricity price periods, the red color represents the peak electricity price periods, and the white color represents the high peak electricity price periods.

It can be observed that the time period of 11:00–13: 00 corresponds to the off-peak electricity price, during which the output of the microgrid units is reduced, the energy storage system is in the charging state, and the power purchased by the microgrid is at its peak. The time period of 19:00–21: 00 corresponds to the peak electricity price, during which the microgrid itself has a relatively small electricity consumption and achieves internal electricity balance through the units and a small amount of energy storage. The time periods of 8:00–11:00 and 13: 00–19:00 both correspond to the high peak electricity price, and the microgrid has a relatively large electricity consumption during these periods. The units have a higher output, and the energy storage system has a negative value, indicating that it is in the discharging state to reduce the amount of electricity purchased by the microgrid. The total cost of the advance economic operation of the microgrid is 48,761.45 yuan, including 27,428.32 yuan for purchased electricity and 21,049.98 yuan for generation costs.

Figure 4 illustrates the operation of Microgrid 1 with a demand response reduction of 600 kW in advance. The red dashed line indicates the demand response period from 15:00 to 17:00. It can be observed that the day-ahead demand response is achieved through the units and energy storage. During the demand response period, the output of the units increases and the energy storage system starts discharging, thereby reducing the power purchased by the microgrid. At this time, the operating cost of the microgrid is 48,794.29 yuan, which is slightly higher compared to the pre-planned cost.
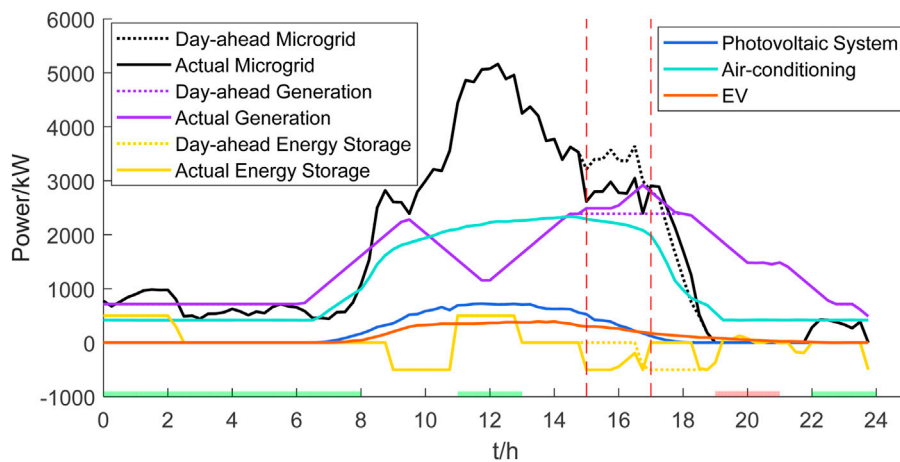
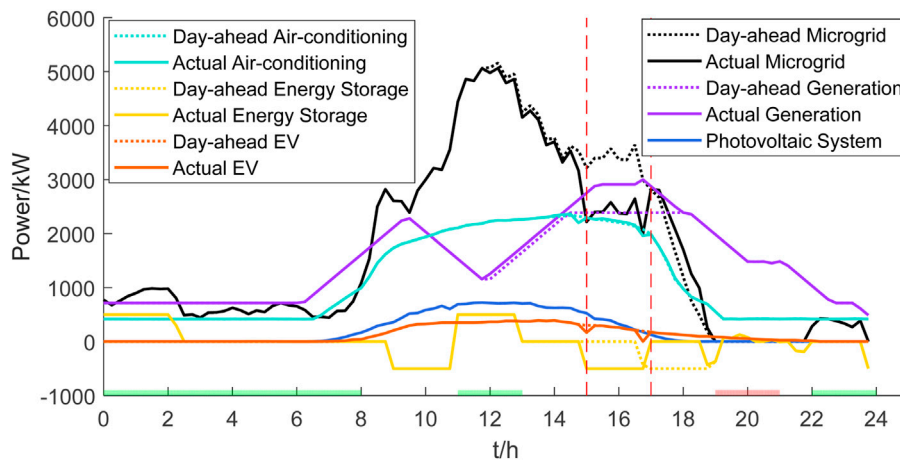**FIGURE 4**
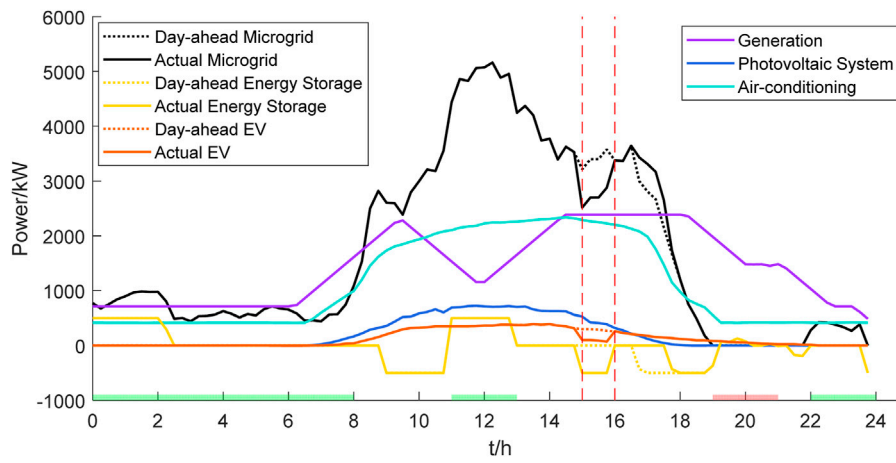Day-ahead demand response reduction of 600 kW of Microgrid 1.

**TABLE 1 Relationship between day-ahead demand response reduction and cost of Microgrid 1.**

| Demand response reduction/kW | 0 | 100 | 200 | 300 | 400 | 500 | 600 | 680 |
|---|---|---|---|---|---|---|---|---|
| Cost in total/yuan | 48,761 | 48,761 | 48,762 | 48,764 | 48,769 | 48,778 | 48,794 | 48,814 |
| Cost of purchased electricity/yuan | 27,428 | 27,420 | 27,396 | 27,331 | 27,231 | 27,099 | 26,856 | 26,636 |
| Generation cost/yuan | 21,050 | 21,058 | 21,083 | 21,150 | 21,255 | 21,397 | 21,656 | 21,895 |



**FIGURE 5**
Hourly demand response reduction of 1,000 kW of Microgrid 1.

Table 1 presents the relationship between the day-ahead demand response reduction and cost for Microgrid 1. It can be observed that as the reduction amount increases, the cost of purchased electricity decreases, while the generation cost increases. At this point, the unit cost of generation is higher than the unit cost of purchased electricity, resulting in an overall increase in the total cost. The maximum demand response reduction for Microgrid 1 during the time period of 15:00–17:00 is 680 kW.

Figure 5 illustrates the operation of Microgrid 1 with an hourly demand response reduction of 1,000 kW. The resources involved in the hourly demand response include units, air conditioning, electric vehicles, and energy storage. As the reduction amount increases, the microgrid first utilizes the energy storage with the lowest cost and starts discharging. Then, the units increase their output. Finally, the electric vehicles and air conditioning, which have higher response costs, are adjusted. The electric vehicles stop charging, and the air

TABLE 2 Relationship between hourly demand response reduction and cost of Microgrid 1.

| Demand response reduction/kW | 0 | 100 | 200 | 300 | 400 | 500 |
|---|---|---|---|---|---|---|
| Cost of purchased electricity and generation/yuan | 48,761 | 48,761 | 48,762 | 48,764 | 48,769 | 48,759 |
| Cost of temperature/yuan | 0.0 | 0.0 | 0.0 | 0.0 | 0.0 | 0.0 |
| Electric vehicle compensation/yuan | 0.0 | 0.0 | 0.0 | 0.0 | 0.0 | 31.5 |
| Demand response reduction/kW | 600 | 700 | 800 | 900 | 1,000 | 1,080 |
| Cost of purchased electricity and generation/yuan | 48,740 | 48,745 | 48,770 | 48,779 | 48,792 | 48,768 |
| Cost of temperature/yuan | 0.0 | 0.0 | 0.0 | 9.3 | 49.3 | 81.3 |
| Electric vehicle compensation/yuan | 84.0 | 102.3 | 102.3 | 144.3 | 178.5 | 283.5 |



FIGURE 6
Minute demand response reduction of 700 kW of Microgrid 1.

TABLE 3 Relationship between minute demand response reduction and the cost of Microgrid 1.

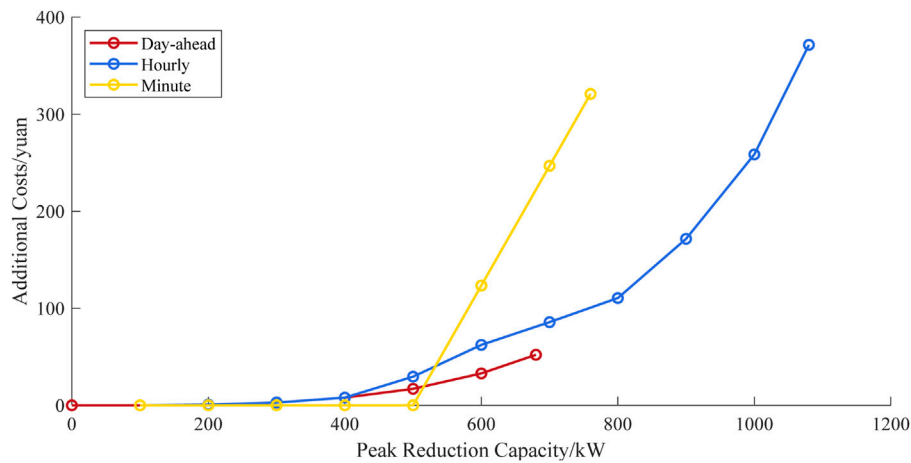| Demand response reduction/kW | 100 | 200 | 300 | 400 | 500 | 600 | 700 | 760 |
|---|---|---|---|---|---|---|---|---|
| Cost of purchased electricity and generation/yuan | 48,761 | 48,761 | 48,761 | 48,761 | 48,761 | 48,675 | 48,588 | 48,536 |
| Electric vehicle compensation/yuan | 0.0 | 0.0 | 0.0 | 0.0 | 0.0 | 210.0 | 420.0 | 546.0 |



FIGURE 7
Curve of relationship between multi-time scale demand response reduction and cost of Microgrid 1.
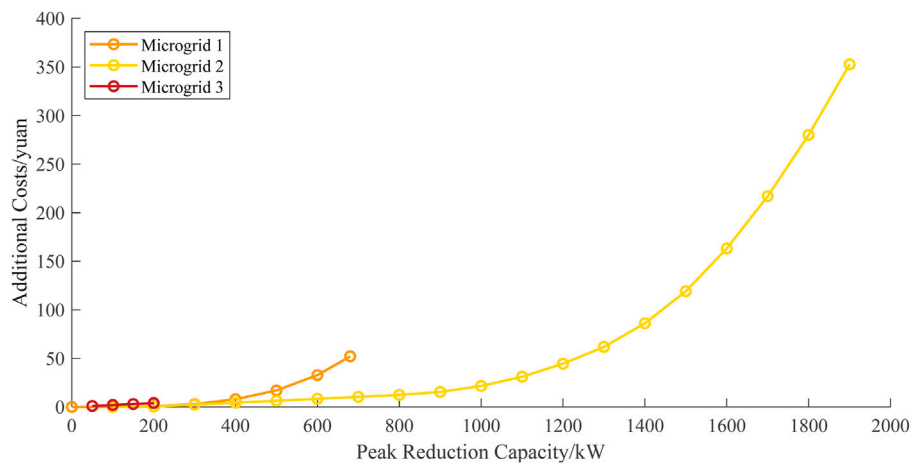
FIGURE 8
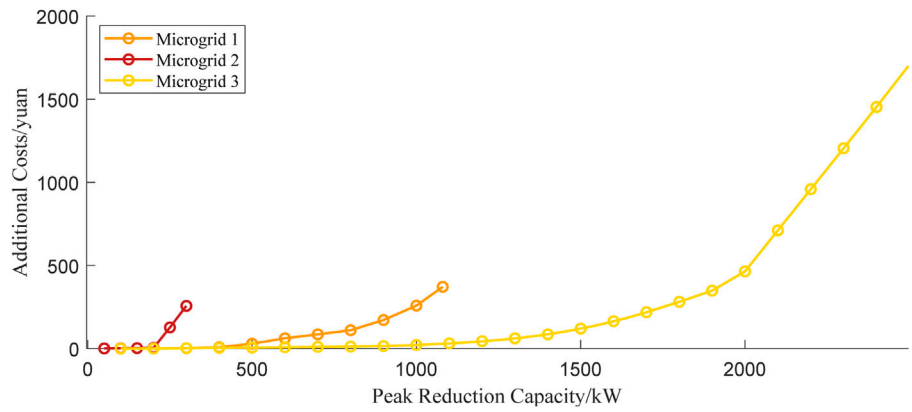Day-ahead scheduling capability of the microgrid.



FIGURE 9
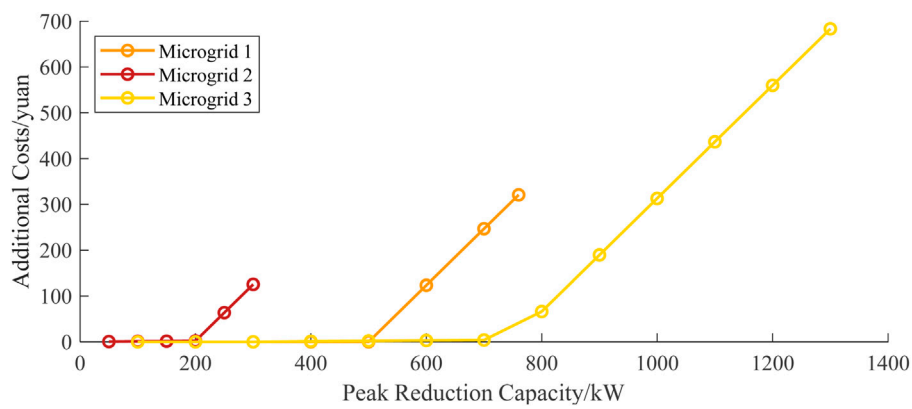Hourly scheduling capability of the microgrid.



FIGURE 10
Minute scheduling capability of the microgrid.

**TABLE 4 Maximum schedulable capacity of the microgrid with multiple time scales.**

| Unit/kW | Microgrid 1 | Microgrid 2 | Microgrid 3 |
|---|---|---|---|
| Day-ahead | 680 | 1,970 | 200 |
| Hourly | 1,080 | 2,530 | 310 |
| Minute | 760 | 1,320 | 315 |
| Second | 242 | 910 | 0 |

conditioning adjusts its output within a small range based on the characteristics of the energy storage.

Table 2 presents the relationship between the hourly demand response reduction and cost for Microgrid 1. It can be observed that as the reduction amount increases, the cost of purchased electricity and generation initially increases, then decreases, and finally increases again. The decrease in the middle is caused by the response of electric vehicles. When the electric vehicles stop charging, the electricity consumption of the microgrid decreases, resulting in a reduction in both the cost of purchased electricity and generation. The maximum hourly demand response reduction for Microgrid 1 during the time period of 15:00–17:00 is 1,080 kW.

Figure 6 illustrates the operation of Microgrid 1 with a minute demand response reduction of 700 kW. The resources involved in the minute demand response are electric vehicles and energy storage. The energy storage discharges, and the electric vehicles stop charging.

Table 3 presents the relationship between the minute demand response reduction and cost for Microgrid 1. As the reduction amount increases, the response from electric vehicles gradually increases, and the compensation from electric vehicles also increases. The maximum minute demand response reduction for Microgrid 1 during the time period of 15:00–17:00 is 760 kW.

Figure 7 illustrates the relationship between the demand response reduction and the corresponding cost increase at multiple time scales for Microgrid 1. It can be observed that there are certain similarities in the demand response across the three time scales. When the reduction amount is less than 500 kW, the cost increase is minimal. However, after the reduction amount exceeds 500 kW, the cost increase shows a clear upward trend.

In addition to these similarities, there are also some differences. In the advance time scale, the dispatchable capacity is relatively small, resulting in lower response costs compared to the hourly scale. In the hourly scale, there is a

greater availability of dispatchable resources and a larger dispatchable capacity. However, this additional capacity comes at the expense of user satisfaction, resulting in relatively higher costs. In the minute scale, the first 500-kW reduction is provided by energy storage with almost no cost. However, the subsequent 260-kW reduction is provided by electric vehicles, resulting in higher costs.

## 5.2 Analysis of demand response in distribution−microgrid coordination

Figures 8–10 represent the day ahead, hourly, and minute dispatching abilities of three microgrids during the time period of 15:00–17:00. These abilities correspond to the relationship between the reduction amount and cost increase. According to the parameters in Supplementary Table SA3, it can be observed that in terms of microgrid loads and various resource magnitudes, Microgrid 2 > Microgrid 1 > Microgrid 3. Correspondingly, at various time scales, the maximum dispatchable capacity of the microgrids follows the order Microgrid 2 > Microgrid 1 > Microgrid 3, as indicated in Table 4. When the reduction quantity is small, the dispatch costs of each microgrid are relatively low. However, with an increase in the reduction quantity, the costs of each microgrid start to rise. Additionally, the marginal dispatch cost becomes larger, and there is a turning point in the reduction quantity, with Microgrid 2 > Microgrid 1 > Microgrid 3.

The hourly level is taken as an example to illustrate the process of demand response between distribution and microgrids. When the distribution network meets the safety constraints of the line and receives instructions from superiors to reduce peak load during the 15:00–17:00 period, only the unit peak load cost of each microgrid is considered. When the peak shaving instructions are 1 MW, 2 MW, and 3 MW, the reduction amounts of microgrid 1, 2, and 3 obtained by solving are shown in Table 5, making the total adjustment cost of the three microgrids the lowest. At this point, the microgrids participating in demand response have similar reduction unit prices. The schedulability of the microgrid is composed of several straight lines between the reduction amount and cost, but in reality, there is not a strict linear relationship. Therefore, the reduction unit prices are not completely consistent, and the error is within an acceptable range.

When the total reduction amount is 3 MW, the demand response curves for the three microgrids are shown in Figures 11–13.

**TABLE 5 Microgrid peak shaving command and corresponding cost.**

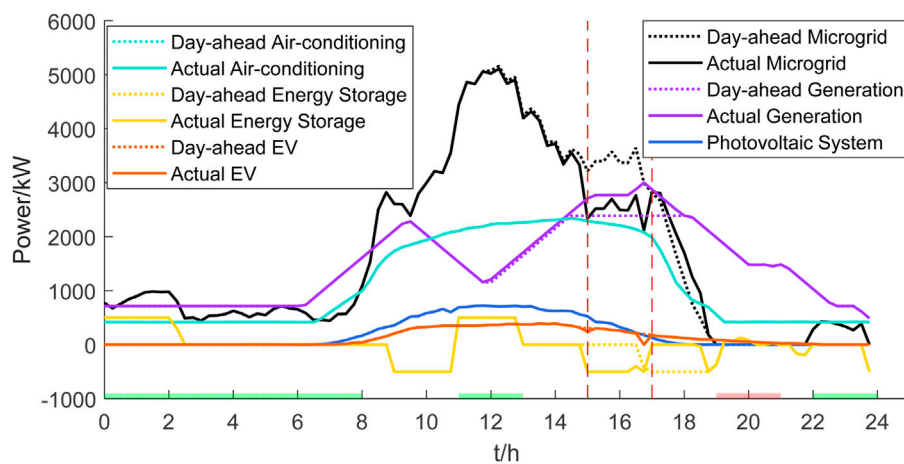| Total reduction amount (MW) | Microgrid 1 | | | Microgrid 2 | | | Microgrid 3 | | |
|---|---|---|---|---|---|---|---|---|---|
| | Reduction amount/ kW | Cost/ yuan | Unit price/ yuan·kW⁻¹ | Reduction amount/ kW | Cost/ yuan | Unit price/ yuan·kW⁻¹ | Reduction amount/ kW | Cost/ yuan | Unit price/ yuan·kW⁻¹ |
| 1 | 346 | 4.75 | 0.01 | 654 | 9.42 | 0.01 | 0 | 0.00 | — |
| 2 | 479 | 23.26 | 0.05 | 1,318 | 65.59 | 0.05 | 203 | 16.30 | 0.08 |
| 3 | 881 | 155.08 | 0.18 | 1,902 | 349.93 | 0.18 | 217 | 51.85 | 0.24 |

**FIGURE 11**
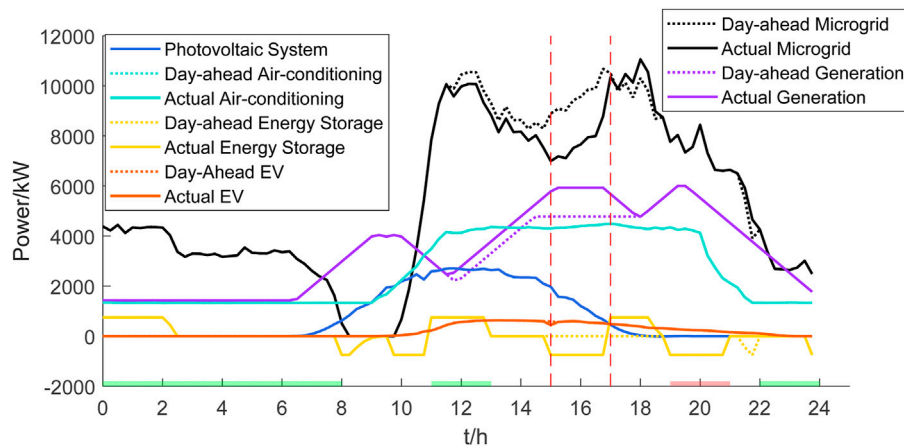Demand response reduction of 881 kW of Microgrid 1.



**FIGURE 12**
Demand response reduction of 1,902 kW of Microgrid 2.

Taking the hourly scale as an example, the process of demand response in distribution–microgrid coordination is explained. When the distribution network operates within the constraints of line safety and receives instructions from the higher-level authority to implement peak shaving during the time period of 15:00–17:00, the focus is on the unit peak shaving cost of each microgrid.

## 6 Conclusion

To improve the scale and frequency of demand response implementation, this paper proposes a coordinated demand response method for distribution–microgrid based on the multi-time scale dispatchable capacity assessment. It is hoped that coordinating distribution and microgrids in a collaborative demand response architecture can enhance the guidance role of the distribution grid in responding to microgrid demands.

Simultaneously, microgrid control strategies should be improved to enable more stable, efficient, and accurate responses, reinforcing the proactive support role of microgrids in the distribution grid. The multi-time scale dispatchable capacity refers to the relationship between the achievable load adjustment and the corresponding cost for demand response at different time scales, including day-ahead, hourly, minute, and second levels. The following conclusion can be drawn:

(1) Different resources are mobilized for demand response at different time scales based on the response characteristics of various load resources. Day-ahead demand response mainly considers the response characteristics of demand-side units and energy storage while meeting the user's energy demand. Hourly demand response, in addition to units and energy storage, also mobilizes air conditioning and electric vehicle resources at the expense of sacrificing some user's energy satisfaction. Minute-level demand
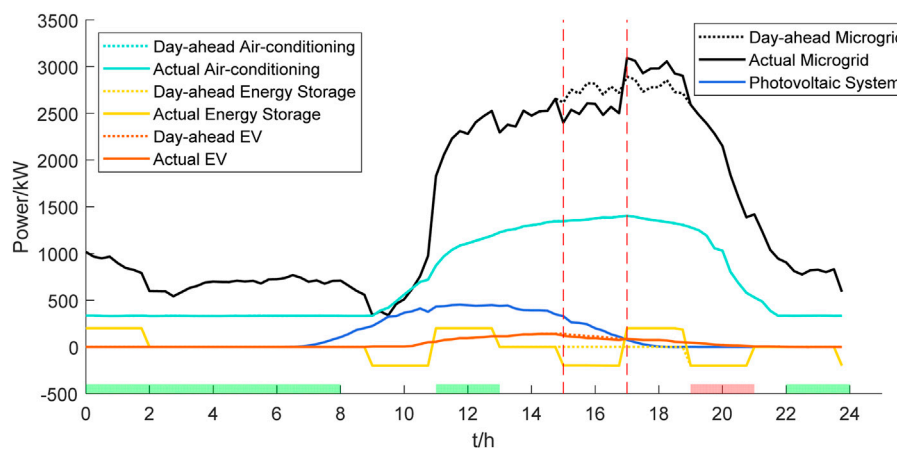
**FIGURE 13**
Demand response reduction of 217 kW of Microgrid 3.

response mobilizes load resources with fast response characteristics such as energy storage and electric vehicles. The second-level demand response corresponds to energy storage and interruptible loads.

(2) The maximum adjustable power and unit adjustment cost at different time scales in the microgrid are different. The overall trend of the maximum adjustable power is as follows: hourly > day-ahead > minute > second; the overall trend of unit adjustment cost is second > minute > hourly > day-ahead, which is consistent with the characteristics of demand response at different time scales.

(3) Through the dispatchable capacity assessment, the distribution network has a clear understanding of the adjustable amount and corresponding cost for each microgrid. With the distribution–microgrid-coordinated demand response architecture, the distribution network can quickly issue instructions, and the microgrid can respond stably and accurately according to the instructions. The coordinated method enables more targeted and frequent demand response on a smaller scale while ensuring the safety constraints of the lines and achieving the lowest total adjustment cost for the microgrid.

However, there are directions for further improvement and enrichment.

(1) Uncertainty in new energy/load forecasting accuracy. The paper currently fully considers the response characteristics of various adjustable resources within the microgrid but does not take into account the impact of factors such as the volatility, randomness, and accuracy of load forecasting on the assessment of microgrid schedulable capacity.

(2) Long-term schedulable capacity assessment. Currently, only the schedulable capacity of microgrids for intraday and intraday is evaluated, without consideration of longer time scales such as "monthly" and "annually." Evaluation of the schedulable capacity within these time frames can have an impact on grid planning.

## Data availability statement

The raw data supporting the conclusion of this article will be made available by the authors, without undue reservation.

## Author contributions

ZX: writing–original draft and writing–review and editing. ZC: writing–original draft and writing–review and editing. HY: writing–original draft and writing–review and editing. DS: writing–original draft and writing–review and editing.

## Funding

## Acknowledgments

## Conflict of interest

Author ZX was employed by State Grid Economic and Technological Research Institute Co., Ltd.

The remaining authors declare that the research was conducted in the absence of any commercial or financial

relationships that could be construed as a potential conflict of interest.

may be evaluated in this article, or claim that may be made by its manufacturer, is not guaranteed or endorsed by the publisher.

## Publisher's note

## Supplementary material

The Supplementary Material for this article can be found online at: https://www.frontiersin.org/articles/10.3389/fenrg.2024.1366859/full#supplementary-material

## References

Alvarez, C., Gabaldon, A., and Molina, A. (2004). Assessment and simulation of the responsive demand potential in end-user facilities application to a university customer. *IEEE Trans. Power Syst.* 19 (2), 1223–1231. doi:10.1109/tpwrs.2004.825878

Belkhier, Y., and Oubelaid, A. (2024). Novel design and adaptive coordinated energy management of hybrid fuel-cells/tidal/wind/PV array energy systems with battery storage for microgrids. *Energy Storage* e556. doi:10.1002/est2.556

Chen, Y. (2021) *Scheduling strategy of power system considering demand response uncertainties*. Master Thesis. China: South China University of Technology.

Cui, Y., Xiu, Z. G., Liu, C., Zhao, Y. T., Tang, Y. H., Chai, X. Z., et al. (2021). Dual level optimal dispatch of power system considering demand response and pricing strategy on deep peak regulation. *Proc. CSEE* 41 (13), 185–193. doi:10.13334/j.0258-8013.pcsee.202105

Dashtdar, M., Belkhier, Y., Bajaj, M., Sadegh, S. M., Belik, M., and Rubanenko, O. (2022). "Protection of DC microgrids based on frequency domain analysis using fourier transform," in 2022 IEEE 3rd KhPI Week on Advanced Technology (KhPIWeek), Kharkiv, Ukraine, October, 2022, 1–6.

Fan, S., Wei, Y. H., He, G. Y., and Li, Z. Y. (2022). Discussion on demand response mechanism for new power systems. *Automation Electr. Power Syst.* 46 (07), 1–12. doi:10.7500/AEPS20210726010

Gan, Z. T. (2022) *Multi-objective scheduling optimization of power system considering demand response under carbon neutral background*. Master Thesis. China: North China Electric Power University.

Gielen, D., Boshell, F., Saygin, D., Bazilian, M. D., Wagner, N., and Gorini, R. (2019). The role of renewable energy in the global energy transformation. *Energy Strategy Rev.* 24, 38–50. doi:10.1016/j.esr.2019.01.006

Hillerbrand, R., Milchram, C., and Schippl, J. (2019). The Capability Approach as a normative framework for technology assessment: capabilities in assessing digitalization in the energy transformation. *TATuP-Z. Für Tech. Theor. Und Prax./J. Technol. Assess. Theory Pract.* 28, 52–57. doi:10.14512/tatup.28.1.52

Huang, M. H., Tang, K. J., Dong, S. F., Nan, B., and Song, Y. H. (2023). Optimal power flow considering user-side carbon emission allowances based on carbon flow theory. *Power Syst. Technol.* 47 (07), 1–10. doi:10.13335/j.1000-3673.pst.2023.0028

Huang, R., and Zhang, S. F. (2020). Practice and enlightenment of power demand-side management in major developed countries. *J. North China Electr. Power Univ.* 6, 47–55. doi:10.14092/j.cnki.cn11-3956/c.2020.06.006

Jiang, X. K. (2018) *Power system optimal operation with large-scale wind power and electric vehicle integrated considering demand response*. Master Thesis. China: Huazhong University of Science and Technology.

Ju, Y. T., and Chen, X. (2023). Distributed active and reactive power coordinated optimal scheduling of networked microgrids based on two-layer multi-agent reinforcement learning. *Proceeding CSEE* 42 (23), 1–16. doi:10.13334/j.0258-8013.pcsee.212737

Kahnamouei, A., and Lotfifard, S. (2022). Enhancing resilience of distribution networks by coordinating microgrids and demand response programs in service restoration. *IEEE Syst. J.* 16 (2), 3048–3059. doi:10.1109/jsyst.2021.3097263

Kang, C. Q., Du, E. S., Li, Y. W., Zhang, N., Chen, Q. X., Guo, H. Y., et al. (2022). Key scientific problems and research framework for carbon perspective research of new power systems. *Power Syst. Technol.* 46 (03), 821–833. doi:10.13335/j.1000-3673.pst.2021.2550

Kong, X. Y., Liu, C., Wang, C. S., Li, S. W., and Chen, S. S. (2022). Demand response potential assessment method based on deep subdomain adaptation network. *Proceeding CSEE* 42 (16), 5786–5797+6156. doi:10.13334/j.0258-8013.pcsee.210903

Li, P. S., Wu, Z. J., Zhang, C., Hu, M. Q., Li, S. F., Wang, F. S., et al. (2021a). Distributed hybrid-timescale voltage/var control in active distribution networks. *Automation Electr. Power Syst.* 45 (16), 160–168. doi:10.7500/AEPS20201225004

Li, W., Han, R. D., Sun, C. J., Fu, P., Zhang, J., Wang, C., et al. (2021b). An optimal incentive contract and strategy of shiftable loads participation in demand response based on user electricity preference. *Proc. CSEE* 41 (S1), 4403–4415. doi:10.13334/j.0258-8013.pcsee.202593

Li, X., Ji, H. S., Zhang, R. F., Jiang, T., Chen, H. H., Ning, R. X., et al. (2022b). Distributed optimal scheduling of urban distribution system considering response

characteristics of multi-type microgrids. *Automation Electr. Power Syst.* 46 (17), 74–82. doi:10.7500/AEPS20220226002

Li, Y. H, and Kong, L. (2019). Developing solar and wind power generation technology to accelerate China's energy transformation. *Bull. Chin. Acad. Sci.* 34, 426–433. doi:10.16418/j.issn.1000-3045.2019.04.007

Li, Y. W., Zhang, N., Du, E. S., Liu, Y. L., Cai, X., He, D. W., et al. (2022a). Mechanism study and benefit analysis on power system low carbon demand response based on carbon emission flow. *Proc. CSEE* 42 (08), 2830–2842. doi:10.13334/j.0258-8013.pcsee.220308

Li, Z. K., Wang, X. X., Shi, S. S., and Zhang, Z. Q. (2022c). Bi-level optimal dispatch of distribution network considering power interaction among microgrids. *South. Power Syst. Technol.* 16 (09), 107–118. doi:10.13648/j.cnki.issn1674-0629.2022.09.013

Li, Z. Y., Wang, G., Ding, M. S., and Wang, L. J. (2017). Demand response potential quantitative evaluation considering load statistical characteristics. *China Sci. Pap.* 12 (05), 529–536. doi:10.3969/j.issn.2095-2783.2017.05.010

Osama, R. A., Zobaa, A. F., and Abdelaziz, A. Y. (2020). A planning framework for optimal partitioning of distribution networks into microgrids. *IEEE Syst. J.* 14 (1), 916–926. doi:10.1109/jsyst.2019.2904319

Wang, B. B., Yang, X. C., and Yang, S. C. (2015). Demand response performance and potential system dynamic analysis based on the long and medium time dimensions. *Proc. CSEE* 35 (24), 6368–6377. doi:10.13334/j.0258-8013.pcsee.2015.24.012

Wang, X. C. (2020) *Research on evaluation method of industrial demand response capacity*. Master Thesis. China: Zhejiang University.

Wang, Y. Q., Qiu, J., Tao, Y. C., and Zhao, J. H. (2020). Carbon-oriented operational planning in coupled electricity and emission trading markets. *IEEE Trans. Power Syst.* 35 (4), 3145–3157. doi:10.1109/tpwrs.2020.2966663

Wei, B. R. (2019) *Research on power system optimal dispatch considering demand response and optimization methods*. Master Thesis. China: Guangxi University.

Xu, C. S. (2021) *Research on Integrated demand response of industrial park*. Master Thesis. China: Zhejiang University.

Xu, Q. S., Ding, Y. F., Yan, Q. G., and Zheng, A. X. (2017). Research on evaluation of scheduling potentials and values on large consumers. *Proc. CSEE* 37 (23), 6791–6800. doi:10.13334/j.0258-8013.pcsee.162638

Xu, Z., Sun, H. B., and Guo, Q. L. (2018). Review and prospect of integrated demand response. *Proceeding CSEE* 38 (24), 7194–7205+7446. doi:10.13334/j.0258-8013.pcsee.180893

Yan, M. Y., Shahidehpour, M., Paaso, A., Zhang, L. X., Alabdulwahab, A., and Abusorrah, A. (2021). Distribution network-constrained optimization of peer-to-peer transactive energy trading among multi-microgrids. *IEEE Trans. Smart Grid* 12 (2), 1033–1047. doi:10.1109/tsg.2020.3032889

Yang, X. F., Su, J., Lv, Z. P., Liu, H. T., and Li, R. (2014). Overview on micro-grid technology. *Proc. CSEE* 34 (01), 57–70. doi:10.13334/j.0258-8013.pcsee.2014.01.007

Yuan, B., Zhang, T. X., and Wang, Y. F. (2022). Study on electric power system operational decision-making with consideration of large scale user load directrix demand response. *Water Resour. Hydropower Eng.* 53 (12), 150–159. doi:10.13928/j.cnki.wrahe.2022.12.016

Zhang, X., Hug, G., Kolter, J. Z., and Harjunkoski, I. (2018). Demand response of ancillary service from industrial loads coordinated with energy storage. *IEEE Trans. Power Syst.* 33 (1), 951–961. doi:10.1109/tpwrs.2017.2704524

Zhang, Z. G., and Kang, C. Q. (2022). Challenges and prospects for constructing the new-type power system towards a carbon neutrality future. *Proc. CSEE* 42 (08), 2806–2819. doi:10.13334/j.0258-8013.pcsee.220467

Zhou, F. Q., Wang, J., Zhao, X. D., and Deng, L. C. (2023). Innovate and optimize power demand response to support the construction of new power system. *Power Demand Side Manag.* 25 (01), 1–4. doi:10.3969/j.issn.1009-1831.2023.01.001

Zhou, X. Q., and Ai, Q. (2020). Combined distributed robust economic dispatch of distribution network and multiple microgrids. *Automation Electr. Power Syst.* 44 (07), 23–30. doi:10.7500/AEPS20190501002